Heliyon 9 (2023) e12540

Contents lists available at ScienceDirect

Heliyon

journal homepage: www.cell.com/heliyon

Research article

Microalgae growth rate multivariable mathematical model for biomass production

Manuel Martinez-Ruiz [a], Karina Vazquez [b], Liliana Losoya [b], Susana Gonzalez [b], Felipe Robledo-Padilla [c], Osvaldo Aquines [c,*], Hafiz M.N. Iqbal [a], Roberto Parra-Saldivar [a,*]

[a] *Tecnologico de Monterrey, School of Engineering and Sciences, Monterrey, 64849, Mexico*
[b] *Department of Biomedical Engineering, Universidad de Monterrey, Av. Morones Prieto 4500, San Pedro Garza García 66238, N.L., Mexico*
[c] *Department of Physics and Mathematics, Universidad de Monterrey, Av. Morones Prieto 4500, San Pedro Garza García 66238, N.L., Mexico*

ARTICLE INFO

Keywords:
Ultraviolet (UV)
Microalgae
Health
Environment
Sunscreen
Amino acid

ABSTRACT

Background: The use of microalgae has been emerging as a potential technology to reduce greenhouse gases and bioremediate polluted water and produce high-value products as pigments, phytohormones, biofuels, and bioactive compounds. The improvement in biomass production is a priority to make the technology implementation profitable in every application mentioned before.
Methods: The present study was conducted to explore the use of microalgae from genus *Chlorella* and *Tetradesmus* for the generation of substances of interest with UV absorption capacity. A mathematical model was developed for both microalgae to characterize the production of microalgae biomass considering the effects of light intensity, temperature, and nutrient consumption. The model was programmed in MATLAB software, where the three parameters were incorporated into a single specific growth rate equation.
Results: It was found that the optimal environmental conditions for each genus (*Chlorella* T=36°C, and I<787 μmol/m^{2}s; *Tetradesmus* T=23°C and I<150 μmol/m^{2}s), as well as the optimal specific growth rate depending on the personalized values of the three parameters.
Conclussion: This work could be used in the production of microalgae biomass for the design and development of topical applications to replace commercial options based on compounds that compromise health and have a harmful impact on the environment.

1. Introduction

Skin damage by solar radiation is a global concern increasing problem [1]. The effects on the skin produced by the effect of this kind of radiation are well known producing damage to DNA, proteins, and lipids. It was reported that this damage can induce early wrinkles, sunburns and evolve to develop diseases like skin cancer. Several cosmetic products have been developed to protect from the harmful effects of solar radiation, meanwhile, the chemical used to reduce the impact of solar radiation also have negative effects on the environment causing coral bleaching and toxic for other marine species. Also, it has been reported that is oxybenzone, the active ingredient in sunscreens, is able to permeate the skin by follicular conduct and achieve vascular system inducing inflammatory effects [1–6].

* Corresponding authors.
E-mail addresses: osvaldo.aquines@udem.edu (O. Aquines), r.parra@tec.mx (R. Parra-Saldivar).

https://doi.org/10.1016/j.heliyon.2022.e12540
Received 20 July 2022; Received in revised form 18 October 2022; Accepted 14 December 2022
Available online 22 December 2022

To combat the sunscreen chemical's harmful effects, several efforts have been reported trying to generate natural sunscreens based on microalgae, which are beneficial for both the ecosystem and humans [7–11]. This is because their photosynthetic activity able to produce compounds as protection mechanisms against UV radiation; such as mycosporine-like amino acids (MAA's) and other carotenoids [12,13]. Comparing several authors, there are some models related to a certain algae's specific growth rate as a function of different parameters [14–21]. Within these models, parameters such as temperature, nutrients, and light intensity were used individually; i.e., they only focused on varying the value of one of these while the others remained constant.

To contribute to the study of microalgae growth and the production of valuable molecules than can be used as UV protectants, a mathematical model was developed focusing in two genus, *Chlorella* and *Tetradesmus*, considering the variables that affecting the microalgae growth, such as light intensity, culture temperature and nutrients concentration. *Chlorella vulgaris* has been reported to have an antioxidant capacity in cells exposed to UV-B rays, stimulating the antioxidant protection mechanism [22]. Also, in the study by Karsten et al. [23], *Chlorella luteoviridis* shows a wide tolerance in growth under all radiation conditions tested (UV-A and UV-B); likewise, UV-absorbing MAA compounds were identified in *Chlorella luteoviridis*. Moreover, *Tetradesmus sp.* has also been used to study pollution and photosynthesis. This microalga has shown resistance to UV-B light and absorption properties against UV-A light under certain conditions. It has different MAA compounds, which give it a level of tolerance to UVA and UVB radiation [24].

2. Material and methods

Starting with the development of the model, the specific growth rate was calculated individually for each of the three parameters (temperature, light intensity, and nutrient consumption) to ensure that the observed behavior was consistent with the literature.

The model was programmed in MATLAB software, where the three parameters were incorporated into a single specific growth rate equation. First, it is necessary for the user to enter the temperature (in the ranges of 23–41 °C for *Chlorella* [25] and 10–35°C for *Tetradesmus* [26]) and the light intensity (in the ranges of 0–2149 μmol/m^{-2}s^{-1} for *Chlorella* [25] and 0–1000 μmol/m^{-2}s^{-1} for *Tetradesmus* [27]).

Once the user enters the values, the model starts by solving Eq. (1). This generates a specific growth rate dependent only on the temperature, where T_{max} is the maximum temperature, T_{min} is the minimum temperature, T_{opt} is the optimum temperature and T is the current temperature of the microalgae. Both Eq. (1) and its parameters are based on the model of [14,15] (Table A.1 and Table A.2).

$$\mu(T) = \frac{(T - T_{\max})(T - T_{\min})^2}{T_{opt} - T_{\min}\left[\left(T_{opt} - T_{\min}\right)\left(T - T_{opt}\right) - \left(T_{opt} - T_{\max}\right)\left(T_{opt} + T_{min} - 2T\right)\right]}. \tag{1}$$

The model then proceeds to calculate the specific growth rate depending on the light intensity by solving Eq. ((2a) and (2b)), which are adapted from the work of [16–18]. Eq. (2a) is used to predict the behavior preceding the saturation point (P_{max}); Eq. (2b) is used for the behavior after the saturation point (P_{max}) because it describes the linear decay from the calculated slope. In these equations, μ_{max} is the maximum specific growth rate, I is the light intensity to which the microalgae is exposed, and K_I is the semisaturation coefficient of the light intensity. This last parameter is normally obtained by physical experimentation; however, the values used in the present model were fitted with the results of [25] for *Chlorella sorokiniana* and [17] for *Tetradesmus obliquus* (Table A.1 and Table A.2).

$$\mu(I) = \begin{cases} \mu(I < P_{max}) = \mu_{max} * \dfrac{I}{K_I + I}, & \text{(a)} \\ \mu(I > P_{max}) = \dfrac{y_2 - y_1}{x_2 - x_1} * I + b. & \text{(b)} \end{cases} \tag{2}$$

Based on the model of [19–21], Eq. (3) was formulated to predict the behavior of the specific growth rate depending only on the concentration of a single nutrient, where N is the concentration of the nutrient and K_N is the nutrient semisaturation constant. The latter was found in the literature separately for *Chlorella* [20] and from *Tetradesmus dimorphus* [28] (for more details, see Table A.1 and Table A.2).

$$\mu(N) = \frac{N}{N + K_N}. \tag{3}$$

To find the total specific growth rate that is reliant on these three parameters, Eq. ((4) and (5)) were used. In these cases, the temperature, light intensity, and nutrient concentration depend on each other, where $\mu(T)$ is the result of Eq. (1), $\mu(I)$ is the result of Eq. ((2a) and (2b)), and $\mu(N)$ is the result of Eq. (3).

$$U1 = \mu(T) * \mu(I), \tag{4}$$

$$U2 = \mu(N) * U1. \tag{5}$$

Having the specific growth rate of the microalgae, a system of equations was created. The first parameter calculated in this system was the biomass, which uses Eq. (6), based on the model of Huesemann et al. [29], where B(t) is the biomass concentration at a specific time, μ is the specific growth rate, and Δt is the change over time (Table A.1 and Table A.2).

$$B(t) = B(t - \Delta t)e^{\mu(\Delta t)}. \tag{6}$$

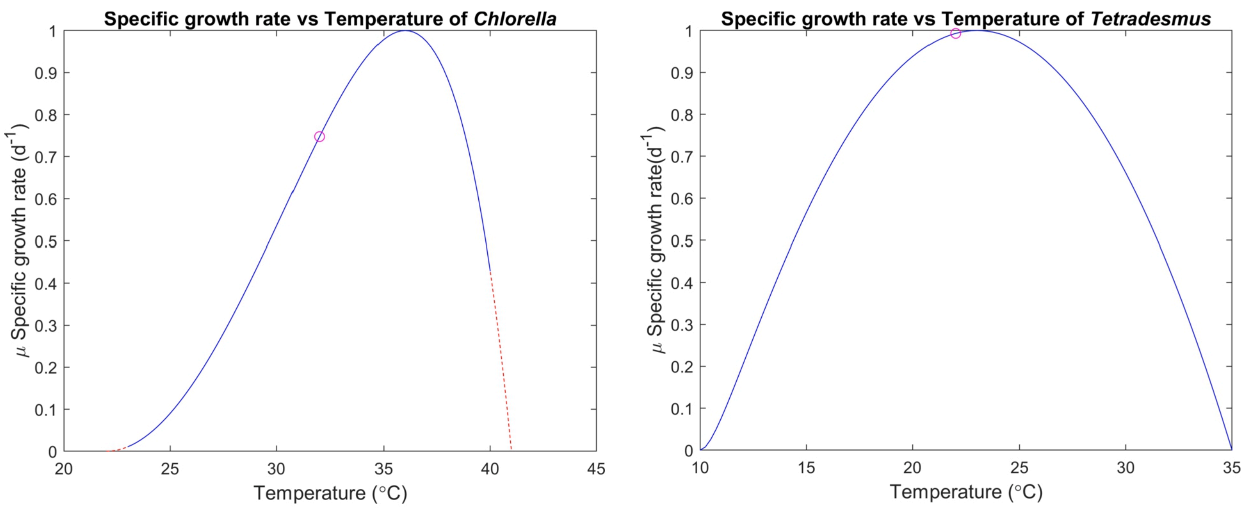

(a) (b)

Figure 1. Plot of temperature vs. specific growth rate: (a) for genus *Chlorella*: a bell shape can be observed on the right side, the red dotted line shows the complete theoretical behavior of the microalgae; (b) for genus *Tetradesmus*: a complete bell curve is observed, this being both its theoretical and experimental behavior; so, a red dotted line was not applied.

Equation (6) was obtained numerically by iterating equations (6) to (10) with 100 time steps, the steps represent 1 hour in days (value: $\Delta t = 0.0416$ day).

For *Chlorella* 85 steps were used and for *Tetradesmus* 100 steps. The steps represent 1 hour in days (value: 0.0416 day).

Knowing the biomass, the system then calculates the behavior of carbon dioxide (CO_2) over time. For this, Eq. (7) is implemented, based on He et al. [30] in which K_{La} is the mass transfer rate, P is the partial pressure of CO_2 in the gas phase, H is Henry's constant of CO_2, $Y_{X/CO2}$ is the yield coefficient of biomass per CO_2 uptake, B is the result of Eq. (6), and CO_2 is the concentration of this dissolved nutrient. To solve Eq. (7), the values of the parameters are shown in Table A.1 and Table A.2.

$$\frac{dCO_2}{dt} = K_{La} * \left(\frac{P}{H} - [CO_2]\right) - Y_{\frac{CO2}{X}} * B(t - \Delta t). \tag{7}$$

To find the yield of each microalgae regarding ammonium (NH_4), it was implemented Eq. (10), which is dependent on Eq. ((8) and (9)) because NO_3 is a secondary product of the consumption of NH_4. For these equations, which are also used by Eze et al. [20], $q_{maxNO3/NH4}$ is the maximum nutrient specific uptake, NO_3 is the liquid phase nitrate concentration, NH_4 is the liquid phase ammonium concentration, CO_2 is the total dissolved inorganic carbon concentration, $K_{N,NO3/NH4}$ is the Monod semi-saturation constant for nutrients, $K_{I,NH4}$ is the Haldane inhibition constant for ammonium, $K_{D,NO3/NH4}$ is the inhibition constant for dissolved inorganic carbon, and B is the result of Eq. (6). These parameters are found in Table A.1 and Table A.2.

$$q_{NO3} = q_{max,NO3} * \frac{[NO_3]}{K_{N,N03} + [NO_3]} * \frac{K_{I,NH4}}{K_{I,NH4} + [NH_4]} * \frac{K_{D,NO3}}{K_{D,NO3} + [CO_2]}, \tag{8}$$

$$q_{NH4} = q_{max,NH4} * \frac{[NH_4]}{K_{N,NH4} + [NH_4] + \frac{[NH_4]^2}{K_{I,NH4}}} * \frac{K_{D,NH4}}{K_{D,NH4} + [CO_2]}, \tag{9}$$

$$\frac{d(NH_4)}{dt} = (q_{NO3} - q_{NH4}) * B(t - \Delta t). \tag{10}$$

Last, Eq. (11) describes the light intensity as a function of the distance from the light source to the algae. This equation is used by different authors, [29,31], in which k_a is the light absorption coefficient, I_0 is the incident light intensity, B is the biomass concentration, and z is the distance between the light source and the microalgae. To resolve Eq. (11), substitute values from Table A.1 and Table A.2.

$$I(z) = I_0 * e^{-k_a B z}. \tag{11}$$

3. Results

To obtain the results, example values for temperature and light intensity for both microalgae were selected. In the case of the present report of results, T=32°C and $I = 1200$ μmol/m^{-2}s^{-1} were selected for *Chlorella*, while for *Tetradesmus*, T=22°C and $I = 840$

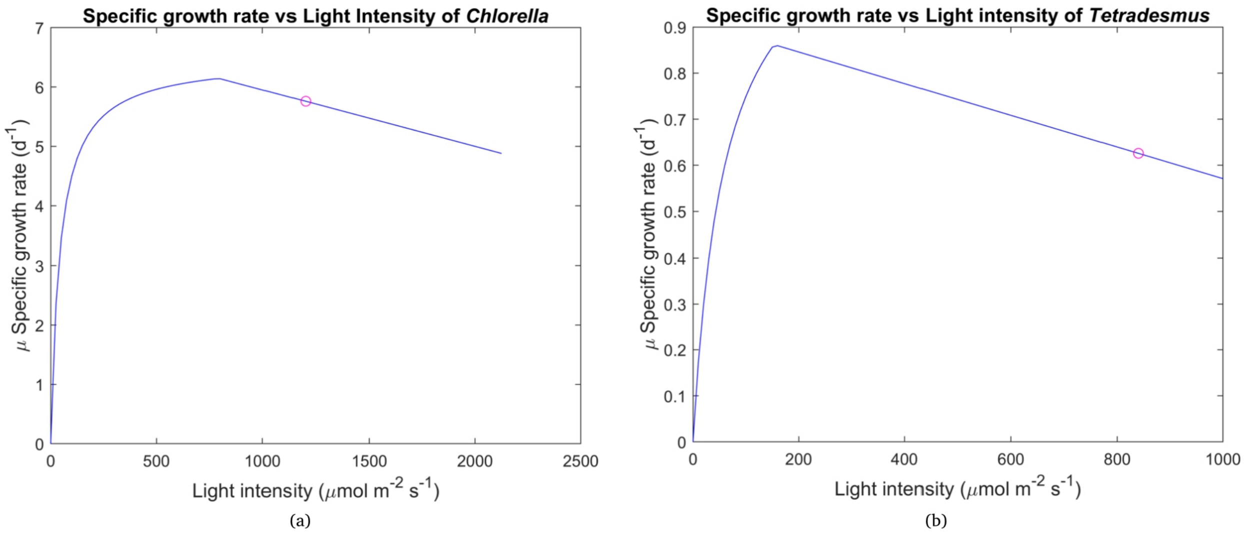

Figure 2. Plot of light intensity vs. specific growth rate for (a) genus *Chlorella* with a saturation point of 787 μmol/$m^{-2}s^{-1}$ and (b) genus *Tetradesmus* with a saturation point of 150 μmol/$m^{-2}s^{-1}$. This theoretical behavior does not take into account the protection mechanisms that will be activated experimentally after the saturation point in the microalgae. Although experimentally this is possible, the algae performance would not be optimal after the saturation point.

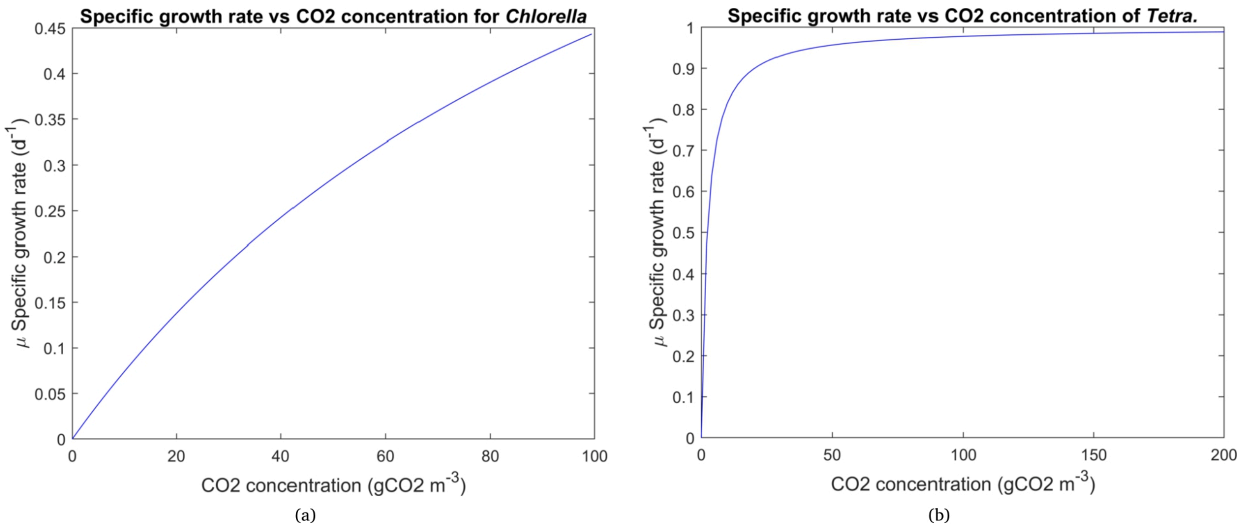

Figure 3. Plot of CO_2 concentration vs. specific growth rate for (a) genus *Chlorella*, this microalgae requires a greater level of CO_2 to saturate; and (b) genus *Tetradesmus*, its specific growth rate is sensitive to changes in CO_2 concentration, saturating at approximately 80 gCO_2m^{-3}. Consequently, *Tetradesmus* become saturated, and its growth rate stops earlier than *Chlorella*.

μmol/$m^{-2}s^{-1}$.

3.1. Parameters for specific growth rate

3.1.1. Temperature

The result of Eq. (1) is shown in Fig. 1(a,b), where the respective temperatures previously selected by the user are shown with a magenta dot. The behavior of the microalgae was due to the habitable temperature range and its optimal temperature.

3.1.2. Light intensity

As mentioned before, the light intensity parameter consists of two equations concerning the saturation point. In the case of *Chlorella*, this point is optimal at $I = 787$ μmol/$m^{-2}s^{-1}$ (data adjusted concerning [25]); meanwhile, for *Tetradesmus*, $I = 150$ μmol/$m^{-2}s^{-1}$ [32].

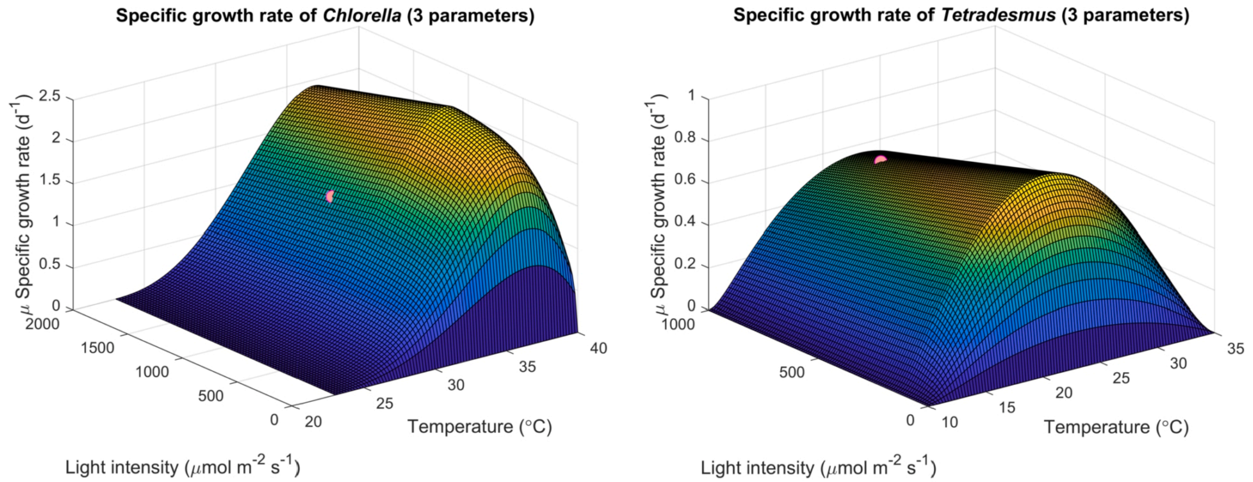

(a) (b)

Figure 4. Graph of Eq. (5) that describes the specific growth rate considering temperature (X-axis), light intensity (Y-axis) and nutrient consumption (Z-axis); the magenta dot is the optimal growth rate for the specific temperature and light intensity the user entered. For (a) genus *Chlorella* ($\mu = 1.276780$ d^{-1}) and (b) genus *Tetradesmus* ($\mu = 0.607284$ d^{-1}).

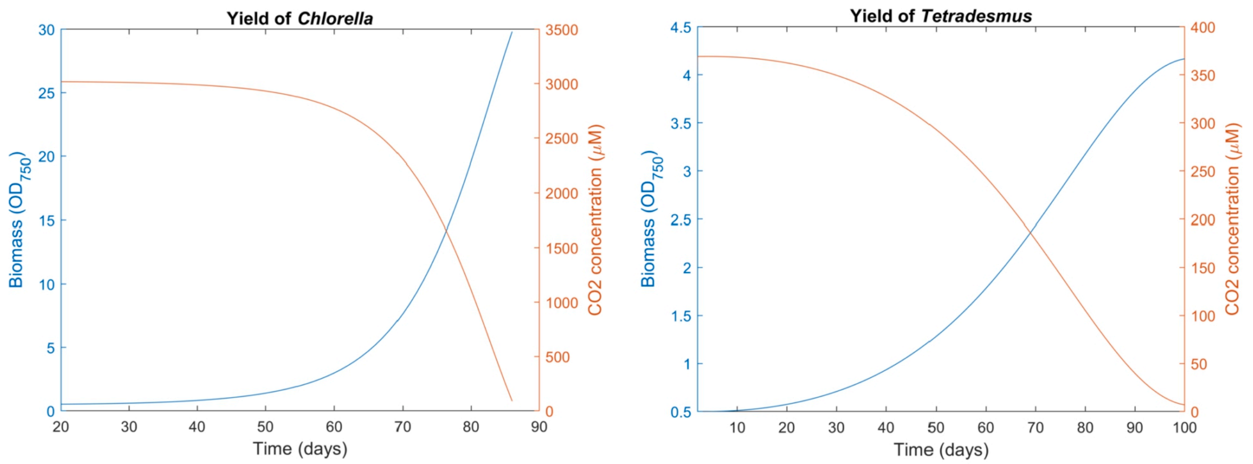

(a) (b)

Figure 5. Yield graph of CO_2 for (a) genus *Chlorella*, where the saturation point is not observed; and (b) genus *Tetradesmus*, which begins to saturate from Day 98 onwards. In both microalgae, the algal biomass increase as CO_2 is consumed. The blue line is the indirect estimated biomass at OD_{750}, and the orange line is the CO_2 concentration.

After saturation point, Eq. (2a) and Eq. (2b) present a decay as a result of photoinhibition, Fig. 2(a,b). Additionally, the light intensities previously selected appear with a magenta marker.

3.1.3. Nutrient consumption

For solving Eq. (3) for both microalgae, it was decided to work with the nutrient CO2 because of its importance in algal photosynthesis. The effects of CO2 on the growth of microalgae are important because it affects the synthetic physiology of algae, modifying their photosynthetic rate and even their saturation point [33]. It was observed that the higher the CO2 concentration was, the higher the growth rate, Fig. 3(a,b).

3.2. Specific growth rate

Eq. (5) describes the specific growth rate for each microalga, Fig. 4(a,b). The 3D graph considers three parameters: temperature (on the X-axis), light intensity (on the Y-axis), and nutrient consumption within the specific growth rate (on the Z-axis), resulting in more realistic behavior.

Additionally, a magenta dot is shown, within Fig. 4(a,b); this indicates the specific growth rate for the value of temperature and

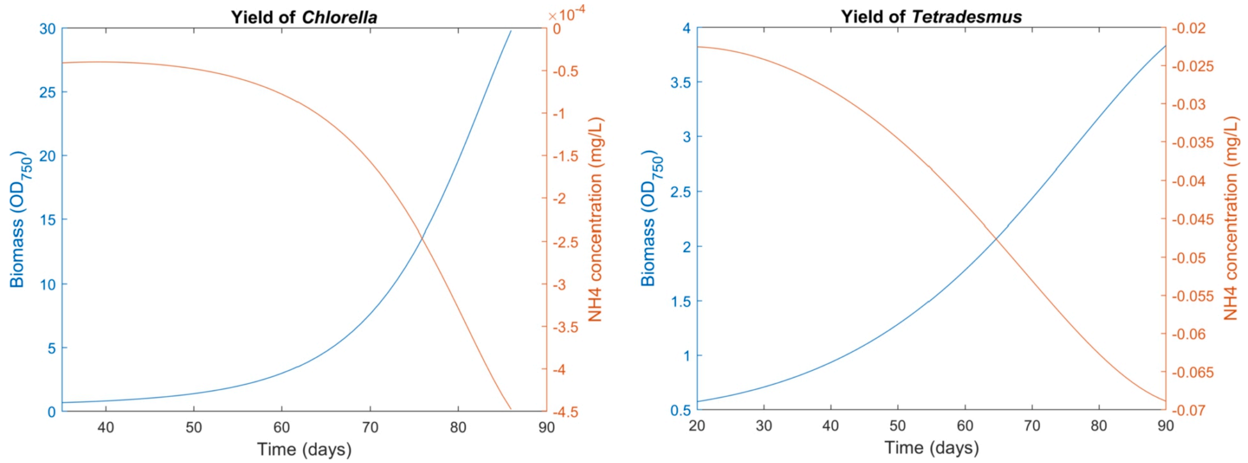

(a) (b)

Figure 6. Yield graph of NH_4 for (a) genus *Chlorella* and (b) genus *Tetradesmus*. In both microalgae, the algal biomass increase as NH_4 is consumed. The blue line is the estimated biomass at OD_{750}, and the orange line is the NH_4 concentration.

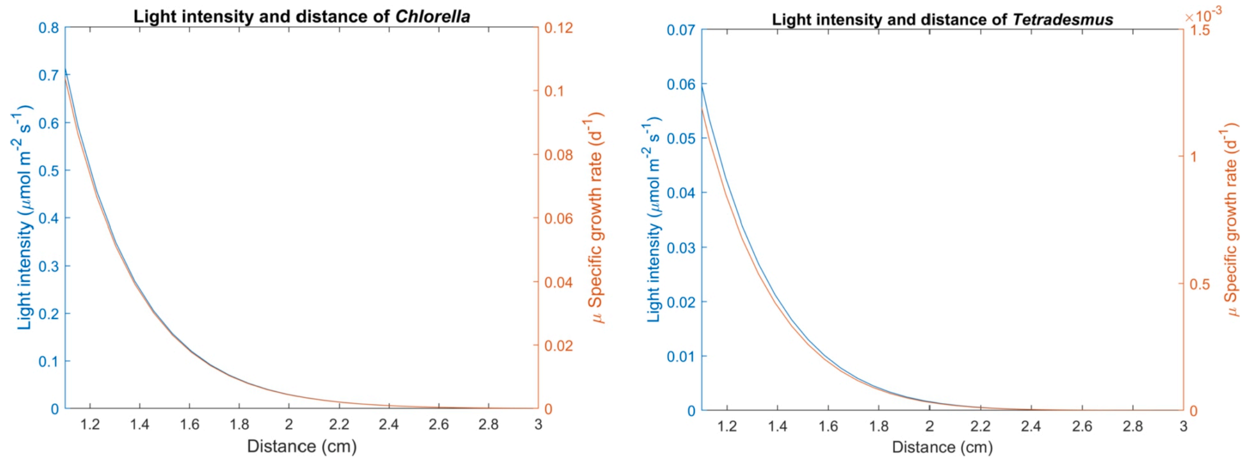

(a) (b)

Figure 7. Plot of light intensity as a function of distance for (a) genus *Chlorella* and (b) genus *Tetradesmus*. The blue line is the light intensity, and the orange line is the specific growth rate. In both cases, the growth rate is greater at higher light intensities and at shorter distances.

light intensity that the user enters at the beginning of the model. For the example given, *Chlorella*, Fig. 4(a), has an optimal value of $\mu = 1.276780\ d^{-1}$, while for *Tetradesmus*, Fig. 4(b), an optimal value of $\mu = 0.607284\ d^{-1}$ is obtained.

3.3. System of equations

3.3.1. Algal biomass and CO_2

To obtain the yield of both microalgae regarding the indirect biomass estimation OD_{750} and CO_2 concentration, Eq. (6) needs to be solved along with Eq. (7), which was solved numerically by time steps previously mentioned, Fig. 5(a,b). The initial biomass is 0.5 [g/m^2-d]) and the remaining parameters were adapted from Table A.1 and Table A.2 of the work of He et al. [30].

In both *Chlorella* and *Tetradesmus*, the biomass starts to grow exponentially as the nutrient is consumed, Fig. 5(a,b); this suggests that they have an inversely proportional behavior. The performance behavior of both microalgae was plotted considering the indirect biomass estimation at OD_{750} (blue line) and the CO_2 concentration in the medium (orange line).

3.3.2. Algal biomass and NH_4

The results obtained from Equations (8)–(10) were plotted to show the behavior of the indirect biomass measure OD_{750} depending on the concentration of ammonium (NH_4) Fig. 6(a,b). When working with two different microalga genus, the parameters used vary due to the naturalness of the microalgae. The same behavior is observed for the nutrient NH_4 as for CO_2 in Fig. 5(a,b). This is because NH_4 and CO_2 are absorbed by the algae for photosynthesis, and in this way, oxygen is generated.

3.3.3. Light intensity and specific growth rate

From results of Eq. (11) for both microalgae, it is appreciated that the behavior is similar, even though the value for each parameter is different, Fig. 7(a,b). This is expected because the light intensity received is high when there is a shorter distance; on the other hand, if the distance increases, the light intensity decreases.

4. Discussion and conclusions

The behavior of the microalgae was characterized using equations that simulate the specific growth rate of the two established microalga genus concerning three parameters. These are the temperature, light intensity, and nutrient consumption; each has its characteristic behavior that affects growth differently.

For growth concerning temperature, the theoretical behavior describes a complete centered bell curve. However, experimentally, it can be in the center, to the left, or the right depending on the habitable temperature range of the microalga, its theoretical optimum temperature, and the experimental optimum temperature. The optimal temperature for Chlorella microalga was found to be 36°C and 23°C for Tetradesmus microalga compared to the existing literature [25,26]. These results, Fig. 1(a,b) followed the pattern proposed by Wong et al. [37], which present less inhibition for temperatures above 25°. Similarly, experimental results of Huesemann et al. [25] show that the optimal specific growth for *Chlorella sorokiniana* is about 35°, which are consistent with the simulation results.

Among the effects of light intensity on algal growth, it was observed that each microalga showed a different saturation point, Fig. 2 (a,b); upon reaching this point, photoinhibition occurred, negatively affecting its photosynthesis process. It was found that the optimal light intensity value for *Chlorella* was less than 787 $\mu mol/m^2$ s (adjusting the data from [25]). Meanwhile, for *Tetradesmus*, it was less than 150 $\mu mol/m^2$ [27]. Huesemann et al. [25] found similar results of the growth rate been stimulated by light intensity until 500 $\mu mol/m^{-2}s^{-1}$ and a very pronounced photoinhibilition after that point.

In the case of nutrient consumption, it was observed that to increase the biomass, the algae must consume the nutrients in the medium, Fig. 3(a,b). Both carbon dioxide (CO_2) [38,39] and ammonium (NH_4) are indispensable for algae growth. The resulting nutrient behavior resembles the investigations by Barajas-Solano et al. [34], which results show growth rates increase with CO2 concentration.

Since there is no model similar to compare the present model, it motivates future work to follow in the direction of a model with the same or other parameters intertwined.

Because of this innovation, the resulting 3D graph, Fig. 4(a,b) predicts a more realistic specific growth rate compared to the existing literature [14–21]. Particularly, the general response of the microalgae agrees with the work of Ota et al. [35].

Therefore, to predict the natural behavior of each microalgae, the specific growth rate was considered a function of these parameters (temperature, light intensity, and nutrient consumption). The results in Fig. 5(a,b) and Fig. 6(a,b) allow the user to predict, through a mathematical model, the behavior of the crop before experimenting physically. These results follows the trend with those of Eze et al. [20]. Moreover, light intensity and growth rate, Fig. 7(a,b) are connected in a similar way predicted by the model of Kim et al. [36].

It will seek to implement this model in the design and creation of topical applications [40–42] with these results; for example, sunscreens based on microalgae can replace commercial alternatives that have a negative effect on both the environment and health.

An area of opportunity within the project is that the use of a closed photobioreactor [43–45] was contemplated, which controls the parameters to generate an optimal growth environment. Additionally, if another parameter (i.e., another equation) is involved, it would be necessary to carry out another extensive investigation where the values of the already existing parameters are not affected; otherwise, it would be necessary to resort to experimentation.

In future work, the model could be adjusted to reflect reality more accurately; to accomplish this, more parameters need to be considered. Examples include pH, glucose, lipids [46], water type and conditions [47–50], secondary nutrients [51–53], and so on [54]. Additionally, because the model is specific for two microalgae (*Chlorella* and *Tetradesmus*), it could be adjusted to become a general model or customized for a larger number of microalgae.

Declarations

Author contribution statement

Manuel Martinez-Rui: Conceived and designed the experiments; Analyzed and interpreted the data; Contributed reagents, materials, analysis tools or data; Wrote the paper.

Karina Vazquez, Liliana Losoya, Susana Gonzalez, Felipe Robledo-Padilla, Osvaldo Aquines: Performed the experiments; Analyzed and interpreted the data; Contributed reagents, materials, analysis tools or data; Wrote the paper.

Hafiz M.N. Iqbal: Analyzed and interpreted the data; Contributed reagents, materials, analysis tools or data; Wrote the paper.

Roberto Parra-Saldivar: Conceived and designed the experiments; Contributed reagents, materials, analysis tools or data; Wrote the paper.

Funding statement

This research did not receive any specific grant from funding agencies in the public, commercial, or not-for-profit sectors.

Data availability statement

The authors do not have permission to share data.

Declaration of interest's statement

The authors declare no competing interests.

Additional information

No additional information is available for this paper.

Appendix A

Table A.1
Equations used in the MATLAB simulations for *Chlorella*.

Model	Parameters	Reference
Eq. (1) $\mu(T) = \frac{(T-T_{\max})(T-T_{\min})^2}{T_{opt}-T_{\min}[(T_{opt}-T_{\min})(T-T_{opt})-(T_{opt}-T_{\max})(T_{opt}+T_{min}-2T)]}$	T_{max}= 41 [°C] T_{min} = 22 [°C] T_{opt} = 36 [°C] T= [23:0.2:40] [°C]	[25] Assigned
Eq. (2a) $\mu(I < P_{max}) = \mu_{max} * \frac{I}{K_I + I}$	I= [0:25:787] [μmol/$m^{-2}s^{-1}$] P_{max} = 787 μmol/$m^{-2}s^{-1}$ μ_{max} = 6.4848 [d^{-1}] K_I = 43.916 [μmol/$m^{-2}s^{-1}$]	Adjusting data with [25] Adjusting data with [25] at T=36°C Adjusting data with [25] at T=36°C Adjusting data with [25] at T=36°C
Eq. (2b) $\mu(I > P_{max}) = \frac{y_2 - y_1}{x_2 - x_1} * I + b$	I= [788:25:2149] [μmol/$m^{-2}s^{-1}$] P_{max} = 787 μmol/$m^{-2}s^{-1}$ $\frac{y_2-y_1}{x_2-x_1} = m = -0.00095$ [μmol/$m^{-2}s^{-1}$-d] b=6.90	Adjusting data with [25] Adjusting data with [25] at T=36°C Adjusting data with [25] at T=36°C Adjusting data with [25] at T=36°C
Eq. (3) $\mu(N) = \frac{N}{N+K_N}$	N_{CO2} = [0:1.17:100] [μM] K_N = 124.9 [mg/L]	[30] [20]
Eq. (6) $B(t) = B(t - \Delta t)e^{\mu(\Delta t)}$	B_0 = 0.5 [g/m2-day] Δt= 0.0416 [days] μ_{max} = 6.4848 [d^{-1}]	[31] Assigned Adjusting data with [25]
Eq. (7) $\frac{dCO_2}{dt} = K_{La} * (\frac{P}{H} - [CO_2]) - Y_{\frac{CO2}{X}} * B(t - \Delta t)$	K_{La} = 17 [d^{-1}] P= 13,000 [Pa] H= 3200 [Pa m^3mol^{-1}] CO_2= [0:1.17:100] [μM] $Y_{x/CO2}$= 100 [mol CO_2/g biomass] B(t-Δt)= Ec. 4	[30] Assigned for Δt= 0.0416 [days] (Ec. 4)
Eq. (8) $q_{NO3} = q_{max,NO3} * \frac{[NO_3]}{K_{N,NO3} + [NO_3]} * \frac{K_{I,NH4}}{K_{I,NH4} + [NH_4]} * \frac{K_{D,NO3}}{K_{D,NO3} + [CO_2]}$ Eq. (9) $q_{NH4} = q_{max,NH4} * \frac{[NH_4]}{K_{N,NH4} + [NH_4] + \frac{[NH_4]^2}{K_{I,NH4}}} * \frac{K_{D,NH4}}{K_{D,NH4} + [CO_2]}$ Eq. (10) $\frac{d(NH_4)}{dt} = (q_{NO3} - q_{NH4}) * B(t - \Delta t)$	$q_{max,NO3}$ = 0.2376 [mgNO_3 d^{-1}] $q_{max,NH4}$= 0.1632 [mgNH_4 d^{-1}] [NO_3]= [0:0.47:40] [mg $L^{-1}d^{-1}$] [NH_4]= [0:1.40:120] [mg $L^{-1}d^{-1}$] CO_2= [0:1.17:100] [μM] $K_{N,NO3}$ = 31.5 mg L^{-1} $K_{N,NH4}$ = 31.5 mg L^{-1} $K_{I,NH4}$ = 0.03 mg L^{-1} $K_{D,NO3}$ = 75.77 mg L^{-1} $K_{D,NH4}$ = 237.18 mg L^{-1} q_{NO3} = Ec. q_{NH4} = Ec. B(t-Δt)= Ec. 4	[21] [20] [20] [30] [20] [21] Adjusting data with [21] Assigned for Δt= 0.0416 [days] (Ec. 4)
Eq. (11) $I(z) = I_0 * e^{-k_a B z}$	I_0 = 25 [μmol/$m^{-2}s^{-1}$] k_a = 6.9557 [μmol/$m^{-2}s^{-1}$] B=B(t-Δt)= Ec. 4 z=[1:0.076:7.5] [cm]	[36] [36] Assigned for Δt= 0.0416 [days] (Ec. 4) [36]

Table A.2
Equations used in the MATLAB simulations for *Scenedesmus*.

Model	Parameters	Reference
Eq. (1)	$T_{max} = 35$ [°C]	[26]
$\mu(T) = \frac{(T-T_{\max})(T-T_{\min})^2}{T_{opt}-T_{\min}[(T_{opt}-T_{\min})(T-T_{opt})-(T_{opt}-T_{\max})(T_{opt}+T_{min}-2T)]}$	$T_{min} = 10$ [°C]	
	$T_{opt} = 23$ [°C]	
	T= [10:0.25:35] [°C]	Assigned
Eq. (2a)	I= 0:10: 150 [µmol/$m^{-2}s^{-1}$]	Adjusting data with [27]
$\mu(I < P_{max}) = \mu_{max}*\frac{I}{K_I+I}$	P_{max}= 150 [µmol/$m^{-2}s^{-1}$]	[32,55]
	K_I= 60.160 [µmol/$m^{-2}s^{-1}$]	Adjusting data with [17]
	$\mu_{max} = 1.2$ [d^{-1}]	[17,55]
Eq. (2b)	I= 151:10:1000 [µmol/$m^{-2}s^{-1}$]	Adjusting data with [27]
$\mu(I > P_{max}) = \frac{y_2-y_1}{x_2-x_1}*I + b$	P_{max}= 150 [µmol/$m^{-2}s^{-1}$]	[32]
	b= 0.9145	Adjusting data with [27] at T= 23°C
	$\frac{y_2-y_1}{x_2-x_1} = m = -0.0003435$ [µmol/$m^{-2}s^{-1}$-d]	Adjusting data with [27] at T= 23°C
Eq. (3)	N_{CO2} = [0:2:200] [µM]	Adjusting data with [33]
$\mu(N) = \frac{N}{N+K_N}$	$K_N = 2.2698$ [gN/m^3]	[28]
Eq. (6)	$B_0 = 0.5$ [g/m^2-day]	[31]
$B(t) = B(t - \Delta t)e^{\mu(\Delta t)}$	Δt= 0.416 [d]	Assigned [17,55]
	$\mu_{max} = 1.2$ [d^{-1}]	
Eq. (7)	$K_{La} = 17$ [d^{-1}]	[30]
$\frac{dCO_2}{dt} = K_{La}*(\frac{P}{H} - [CO_2]) - Y_{\frac{CO2}{X}}*B(t - \Delta t)$	P= 13,000 [Pa]	[30]
	H= 3200 [Pa m^3mol^{-1}]	[30]
	S= CO_2= [0:2:200] [µM]	Adjusting data with [33]
	$Y_{S/x}$= 100 [mol CO_2/g biomass]	[30]
	B= B(t-Δt)= Ec. 4	Assigned for Δt= 0.0416 [days] (Ec. 4)
Eq. (8)	$q_{max,NO3} = 0.2376$ [mgNO_3 d^{-1}]	[21]
$q_{NO3} = q_{max,NO3}*\frac{[NO_3]}{K_{N,N03}+ [NO_3]}*\frac{K_{I,NH4}}{K_{I,NH4}+[NH_4]}*\frac{K_{D,NO3}}{K_{D,NO3}+[CO_2]}$	$q_{max,NH4} = 0.1632$ [mg$NH_4$$d^{-1}$]	
Eq. (9)	[NO_3] = [0:0.5:51] [mg $L^{-1}d^{-1}$]	[56]
$q_{NH4} = q_{max,NH4}*\frac{[NH_4]}{K_{N,NH4}+ [NH_4]+\frac{[NH_4]^2}{K_{I,NH4}}}*\frac{K_{D,NH4}}{K_{D,NH4}+[CO_2]}$	[NH_4] = [40:1.19:160] [mg $L^{-1}d^{-1}$]	[57]
Eq. (10)	CO_2 = [0:2:200] [µM]	Adjusting data with [33]
$\frac{d(NH_4)}{dt} = (q_{NO3} - q_{NH4})*B(t - \Delta t)$	$K_{N,NO3} = 31.5$ mg L^{-1}	[20]
	$K_{N,NH4} = 31.5$ mg L^{-1}	
	$K_{I,NH4} = 39.14$ mg L^{-1}	Adjusting data with [21]
	$K_{D,NO3} = 30$ mg L^{-1}	
	$K_{D,NH4} = 350$ mg L^{-1}	
	q_{NO3} = Ec. 9	Adjusting data with [21]
	q_{NH4} = Ec. 10	
	B(t-Δt) = Ec. 4	Assigned for Δt= 0.0416 [days] (Ec. 4)
Eq. (11)	$I_o = 2.170$ [µmol/$m^{-2}s^{-1}$]	[36]
$I(z) = I_0*e^{-k_aBz}$	k_a= 6.9557 µmol/$m^{-2}s^{-1}$	[36]
	B= B(t-Δt)	Assigned for Δt= 0.0416 [days] (Ec. 4)
	z= [1:0.065:7.5] [cm]	[36]

References

[1] F. Liu-Smith, J. Jia, Y. Zheng, UV-induced molecular signaling differences in melanoma and non-melanoma skin cancer, Adv. Exp. Med. Biol. 996 (2017) 27–40.
[2] N. Saewan, A. Jimtaisong, Natural products as photoprotection, J. Cosmet. Derm. 14 (2015) 47–63.
[3] T.L. de Jager, A.E. Cockrell, S.S. Du Plessis, Ultraviolet light induced generation of reactive oxygen species BT, in: S.I. Ahmad (Ed.), Ultraviolet Light in Human Health, Diseases and Environment, Springer International Publishing, Cham, 2017, pp. 15–23.
[4] A. Siller, S.C. Blaszak, M. Lazar, E. Olasz Harken, Update about the effects of the sunscreen ingredients oxybenzone and octinoxate on humans and the environment. plast, Aesthetic Nurs. (2019) 39.
[5] A. Carvalhais, B. Pereira, M. Sabato, R. Seixas, M. Dolbeth, A. Marques, S. Guilherme, P. Pereira, M. Pacheco, C. Mieiro, Mild effects of sunscreen agents on a marine flatfish: oxidative stress, energetic profiles, neurotoxicity and behaviour in response to titanium dioxide nanoparticles and oxybenzone, Int. J. Mol. Sci. (2021) 22.
[6] N.R. Pilli, S. Narayanasamy, J. Florian, R. Zusterzeel, V. Patel, D.G. Strauss, M.K. Matta, Novel simultaneous method for the determination of avobenzone and oxybenzone in human plasma by UHPLC-MS/MS with phospholipid removal pretreatment: an application to a sunscreen clinical trial, J. Chromatogr. B 1169 (2021), 122615.
[7] T.J. Baker, C.R. Tyler, T.S. Galloway, Impacts of metal and metal oxide nanoparticles on marine organisms, Environ. Pollut. 186 (2014) 257–271.
[8] R.K. Cross, C. Tyler, T.S. Galloway, Transformations that affect fate, form and bioavailability of inorganic nanoparticles in aquatic sediments, Environ. Chem. 12 (2015) 627–642.
[9] G.E. Schaumann, A. Philippe, M. Bundschuh, G. Metreveli, S. Klitzke, D. Rakcheev, A. Grün, S.K. Kumahor, M. Kühn, T. Baumann, et al., Understanding the fate and biological effects of Ag- and TiO2-nanoparticles in the environment: the quest for advanced analytics and interdisciplinary concepts, Sci. Total Environ. 535 (2015) 3–19.
[10] The trouble with ingredients in sunscreens | EWG's Guide to Sunscreens Available online: https://www.ewg.org/sunscreen/report/the-trouble-with-sunscreen-chemicals/. (Accessed 3 January 2021).

[11] NOAA researchers discover sunscreen chemicals threaten corals and other marine life, Available online: https://www.positivelyosceola.com/noaa-researchers-discover-sunscreen-chemicals-threaten-corals-and-other-marine-life/. (Accessed 20 December 2020).
[12] J. Kováčik, B. Klejdus, M. Bačkor, Physiological responses of scenedesmus quadricauda (Chlorophyceae) to UV-A and UV-C light, Photochem. Photobiol. 86 (2010) 612–616.
[13] K.P. Lawrence, P.F. Long, A.R. Young, Mycosporine-like amino acids for skin photoprotection, Curr. Top. Med. Chem. 25 (2018) 5512–5527.
[14] O. Bernard, B. Rémond, Validation of a simple model accounting for light and temperature effect on microalgal growth, Bioresour. Technol. 123 (2012) 520–527.
[15] G. Randrianarison, M.A. Ashraf, J.W. Lee, D.M. Day, L.D. Kapoor, L.D. Kapoor, Q. Béchet, A. Shilton, B. Guieysse, Modeling the effects of light and temperature on algae growth, Biotechnol. Adv. 31 (2013) 19–40.
[16] J.C.M. Pires, A.L. Gonçalves, F.G. Martins, M.C.M. Alvim-Ferraz, M. Simões, Effect of light supply on CO2 capture from atmosphere by Chlorella vulgaris and Pseudokirchneriella subcapitata, Mitig. Adapt. Strategies Glob. Change 19 (2014) 1109–1117.
[17] J. Zambrano, I. Krustok, E. Nehrenheim, B. Carlsson, A simple model for algae-bacteria interaction in photo-bioreactors, Algal Res. 19 (2016) 155–161.
[18] M.N. Metsoviti, G. Papapolymerou, I.T. Karapanagiotidis, N. Katsoulas, Effect of light intensity and quality on growth rate and composition of Chlorella vulgaris, Plants 9 (2020) 1–17.
[19] A. Solimeno, Numerical Modelling of Microalgae Systems for Wastewater Treatment, Univeristat Politècnica de Catalunya·Barcelona Tech, 2017.
[20] V.C. Eze, S.B. Velasquez-Orta, A. Hernández-García, I. Monje-Ramírez, M.T. Orta-Ledesma, Kinetic modelling of microalgae cultivation for wastewater treatment and carbon dioxide sequestration, Algal Res. 32 (2018) 131–141.
[21] L.F. Saldarriaga, F. Almenglo, M. Ramírez, D. Cantero, Kinetic characterization and modeling of a microalgae consortium isolated from landfill leachate under a high CO2 concentration in a bubble column photobioreactor, Electron. J. Biotechnol. 44 (2020) 47–57.
[22] G. Malanga, S. Puntarulo, Oxidative stress and antioxidant content in Chlorella vulgaris after exposure to ultraviolet-B radiation, Physiol. Plant. 94 (1995) 672–679.
[23] U. Karsten, S. Lembcke, R. Schumann, The effects of ultraviolet radiation on photosynthetic performance, growth and sunscreen compounds in aeroterrestrial biofilm algae isolated from building facades, Planta 225 (2007) 991–1000.
[24] F. Xiong, J. Kopecky, L. Nedbal, The occurrence of UV-B absorbing mycosporine-like amino acids in freshwater and terrestrial microalgae (Chlorophyta), Aquat. Bot. 63 (1999) 37–49.
[25] M. Huesemann, B. Crowe, P. Waller, A. Chavis, S. Hobbs, S. Edmundson, M. Wigmosta, A validated model to predict microalgae growth in outdoor pond cultures subjected to fluctuating light intensities and water temperatures, Algal Res. 13 (2016) 195–206.
[26] C.E. Andrade, A.L. Vera, C.H. Cárdenas, E.D. Morales, Biomass production of microalga Scenedesmus sp. with wastewater from fishery, Rev. Téc. Fac. Ing., Univ. Zulia 32 (2009) 126–134.
[27] B. Gris, T. Morosinotto, G.M. Giacometti, A. Bertucco, E. Sforza, Cultivation of Scenedesmus obliquus in photobioreactors: effects of light intensities and light-dark cycles on growth, productivity, and biochemical composition, Appl. Biochem. Biotechnol. 172 (2014) 2377–2389.
[28] R. Chandra, D. Goswami, E. Biotech, Scenedesmus dimorphus and Scenedesmus quadricauda: two potent indigenous microalgae strains for biomass production and CO2 mitigation - a study on their growth behavior and lipid productivity under different concentration of urea as nitrogen source, J. Algal Biomass Utln. 2 (2011) 42–49.
[29] M.H. Huesemann, J. Van Wagenen, T. Miller, A. Chavis, S. Hobbs, B. Crowe, A screening model to predict microalgae biomass growth in photobioreactors and raceway ponds, Biotechnol. Bioeng. 110 (2013) 1583–1594.
[30] L. He, V.R. Subramanian, Y.J. Tang, Experimental analysis and model-based optimization of microalgae growth in photo-bioreactors using flue gas, Biomass Bioenergy 41 (2012) 131–138.
[31] W. Blanken, P.R. Postma, L. de Winter, R.H. Wijffels, M. Janssen, Predicting microalgae growth, Algal Res. 14 (2016) 28–38.
[32] E. Sforza, B. Gris, C.E. De Farias Silva, T. Morosinotto, A. Bertucco, Effects of light on cultivation of scenedesmus obliquus in batch and continuous flat plate photobioreactor, Chem. Eng. Trans. 38 (2014) 211–216.
[33] Y. Yang, K. Gao, Effects of CO2 concentrations on the freshwater microalgae, Chlamydomonas reinhardtii, Chlorella pyrenoidosa and Scenedesmus obliquus (Chlorophyta), J. Appl. Phycol. 15 (2003) 379–389.
[34] A.F. Barajas-Solano, C.A. Godoy-Ruiz, J.D. Monroy-Davila, C. Barajas-Ferreira, V. Kafarov, Mejoramiento del secuestro de CO 2 por Chlorella vulgaris UTEX 1803 en fotobiorreactores a escala laboratorio Improvement of CO 2 sequestration by Chlorella vulgaris UTEX 1803 on labscale photobioreactors, Rev. ION 25 (2012) 39–47.
[35] M. Ota, M. Takenaka, Y. Sato, R. Lee Smith, H. Inomata, Effects of light intensity and temperature on photoautotrophic growth of a green microalga, Chlorococcum littorale, Biotechnol. Rep. 7 (2015) 24–29.
[36] N.J. Kim, I.S. Suh, B.K. Hur, C.G. Lee, Simple monodimensional model for linear growth rate of photosynthetic microorganisms in flat-plate photobioreactors, J. Microbiol. Biotechnol. 12 (2002) 962–971.
[37] C.Y. Wong, M.L. Teoh, S.M. Phang, P.E. Lim, J. Beardall, Interactive effects of temperature and uv radiation on photosynthesis of chlorella strains from polar, temperate and tropical environments: differential impacts on damage and repair, PLoS ONE 10 (2015) 1–14.
[38] Y. Chen, C. Xu, How to narrow the CO2 gap from growth-optimal to flue gas levels by using microalgae for carbon capture and sustainable biomass production, J. Clean. Prod. 280 (2021), 124448.
[39] C. Song, Y. Qiu, S. Li, Z. Liu, G. Chen, L. Sun, K. Wang, Y. Kitamura, A novel concept of bicarbonate-carbon utilization via an absorption-microalgae hybrid process assisted with nutrient recycling from soybean wastewater, J. Clean. Prod. 237 (2019), 117864.
[40] C. Park, K. Heo, S. Oh, S.B. Kim, S.H. Lee, Y.H. Kim, Y. Kim, J. Lee, S.O. Han, S.W. Lee, et al., Eco-design and evaluation for production of 7-aminocephalosporanic acid from carbohydrate wastes discharged after microalgae-based biodiesel production, J. Clean. Prod. 133 (2016) 511–517.
[41] G. Deviram, T. Mathimani, S. Anto, T.S. Ahamed, D.A. Ananth, A. Pugazhendhi, Applications of microalgal and cyanobacterial biomass on a way to safe, cleaner and a sustainable environment, J. Clean. Prod. 253 (2020), 119770.
[42] M.P. Sudhakar, B.R. Kumar, T. Mathimani, K. Arunkumar, A review on bioenergy and bioactive compounds from microalgae and macroalgae-sustainable energy perspective, J. Clean. Prod. 228 (2019) 1320–1333.
[43] K. Azizi, M. Keshavarz Moraveji, H. Hassanzadeh, H. Abedini Najafabadi, Consideration of inclined mixers embedded inside a photobioreactor for microalgae cultivation using computational fluid dynamic and particle image velocimetry measurement, J. Clean. Prod. 195 (2018) 753–764.
[44] B.R. de A. Moreira, Y. Araujo Frias, E. Wilson de Lima, V.H. Cruz, P.R. Matos Lopes, R. da S. Viana, Algae-specific colorful LEDs: biotechnological drivers to biorefinery and photobiological platforms, J. Clean. Prod. (2021) 316.
[45] A. Viruela, Á. Robles, F. Durán, M.V. Ruano, R. Barat, J. Ferrer, A. Seco, Performance of an outdoor membrane photobioreactor for resource recovery from anaerobically treated sewage, J. Clean. Prod. 178 (2018) 665–674.
[46] X.B. Tan, X.C. Zhao, L. Yang, Bin strategies for enhanced biomass and lipid production by Chlorella pyrenoidosa culture in starch processing wastewater, J. Clean. Prod. 236 (2019), 117671.
[47] C. Song, X. Hu, Z. Liu, S. Li, Y. Kitamura, Combination of brewery wastewater purification and CO2 fixation with potential value-added ingredients production via different microalgae strains cultivation, J. Clean. Prod. 268 (2020), 122332.
[48] A.C.C. Pena, C.B. Agustini, L.F. Trierweiler, M. Gutterres, Influence of period light on cultivation of microalgae consortium for the treatment of tannery wastewaters from leather finishing stage, J. Clean. Prod. 263 (2020), 121618.
[49] J. Lv, B. Guo, J. Feng, Q. Liu, F. Nan, X. Liu, S. Xie, Integration of wastewater treatment and flocculation for harvesting biomass for lipid production by a newly isolated self-flocculating microalga Scenedesmus rubescens SX, J. Clean. Prod. 240 (2019), 118211.
[50] A. Sepehri, M.H. Sarrafzadeh, M. Avateffazeli, Interaction between Chlorella vulgaris and nitrifying-enriched activated sludge in the treatment of wastewater with low C/N ratio, J. Clean. Prod. 247 (2020), 119164.

[51] J. Abraham, Y. Lin, A. RoyChowdhury, C. Christodoulatos, M. Conway, B. Smolinski, W. Braida, Algae toxicological assessment and valorization of energetic-laden wastewater streams using Scenedesmus obliquus, J. Clean. Prod. 202 (2018) 838–845.

[52] N. Rashid, M. Nayak, B. Lee, Y.K. Chang, Efficient microalgae harvesting mediated by polysaccharides interaction with residual calcium and phosphate in the growth medium, J. Clean. Prod. 234 (2019) 150–156.

[53] X. Quan, R. Hu, H. Chang, X. Tang, X. Huang, C. Cheng, N. Zhong, L. Yang, Enhancing microalgae growth and landfill leachate treatment through ozonization, J. Clean. Prod. 248 (2020), 119182.

[54] E. Koutra, S.G. Mastropetros, S.S. Ali, K. Tsigkou, M. Kornaros, Assessing the potential of Chlorella vulgaris for valorization of liquid digestates from agro-industrial and municipal organic wastes in a biorefinery approach, J. Clean. Prod. 280 (2021), 124352.

[55] A. Solimeno, R. Samsó, E. Uggetti, B. Sialve, J.P. Steyer, A. Gabarró, J. García, New mechanistic model to simulate microalgae growth, Algal Res. 12 (2015) 350–358.

[56] E.G. Pereira, M.A. Martins, M.D.S.A. Mendes, L.B.B. Mendes, A.N. Nesi, Outdoor cultivation of Scenedesmus obliquus BR003 in stirred tanks by airlift, Eng. Agric. 37 (2017) 1041–1055.

[57] M. Kisielewska, M. Zielinski, M. Debowski, J. Kazimierowicz, Z. Romanowska-Duda, M. Dudek, Effectiveness of Scenedesmus sp. biomass grow and nutrients removal from liquid phase of digestates, Energies 13 (2020) 1–11.